Supplemental Materials

Molecular Biology of the Cell

Vishnu et al.

Figure S1

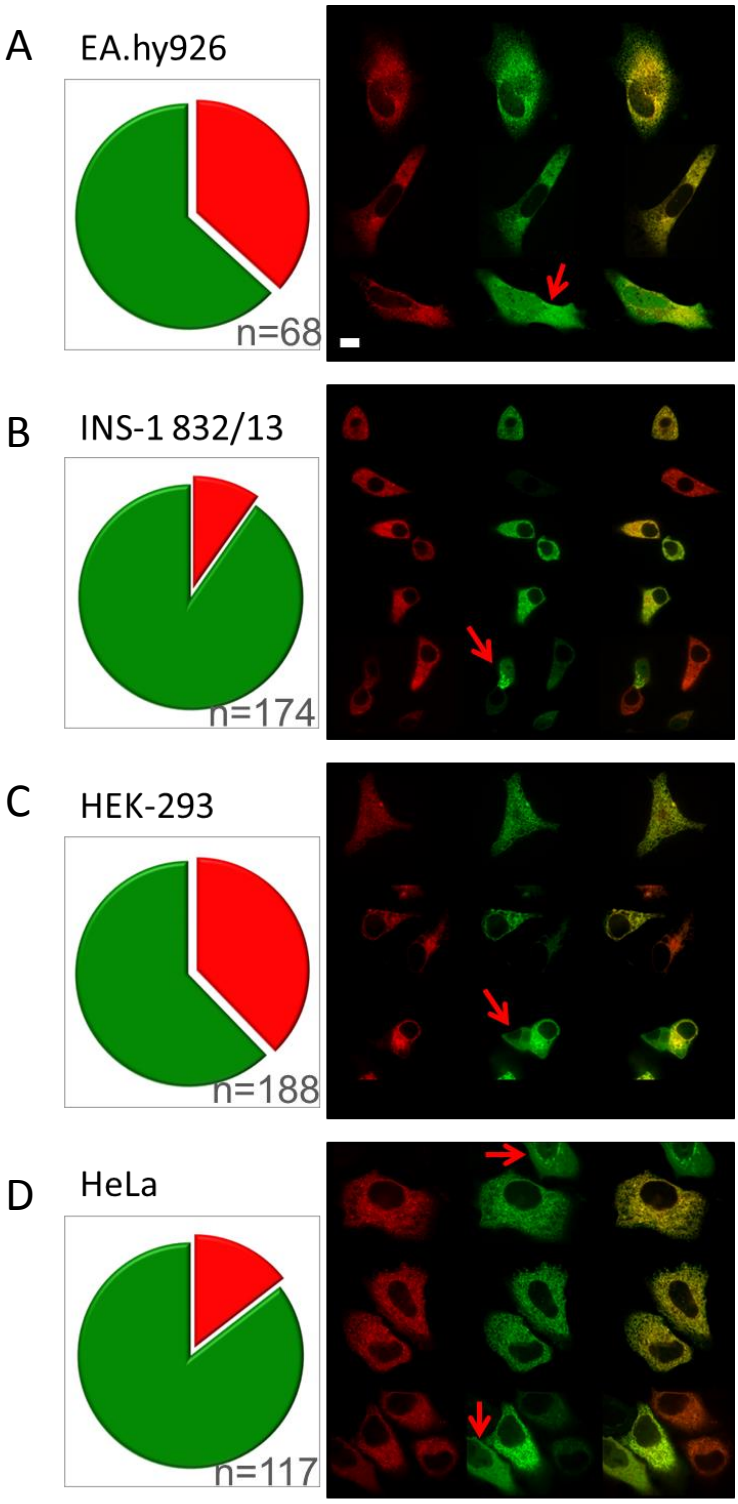

Localization of ERAT4.01 in different cell types

High resolution confocal microscopy was used to investigate the localization of ERAT4.01 in the 4 different cell types, EA.hy926 (panel A), INS-1 832/13 (panel B), HEK-293 (panel C), and HeLa cells (panel D). Cells expressing both ER targeted RFP (ER-RFP) and ERAT4.01 were imaged. Representative images of cells expressing ER-RFP (red cells) and ERAT4.01 (green cells) and respective overlays are presented in the right panel. The white bar in the upper image represents 10 µm. Red arrows indicate cells with a clear mistargeting of the ER ATP probe. Diagrams in the left panel represent the proportion of cells with correct targeted (green) and mistargeted ERAT4.01 (red).

Figure S2

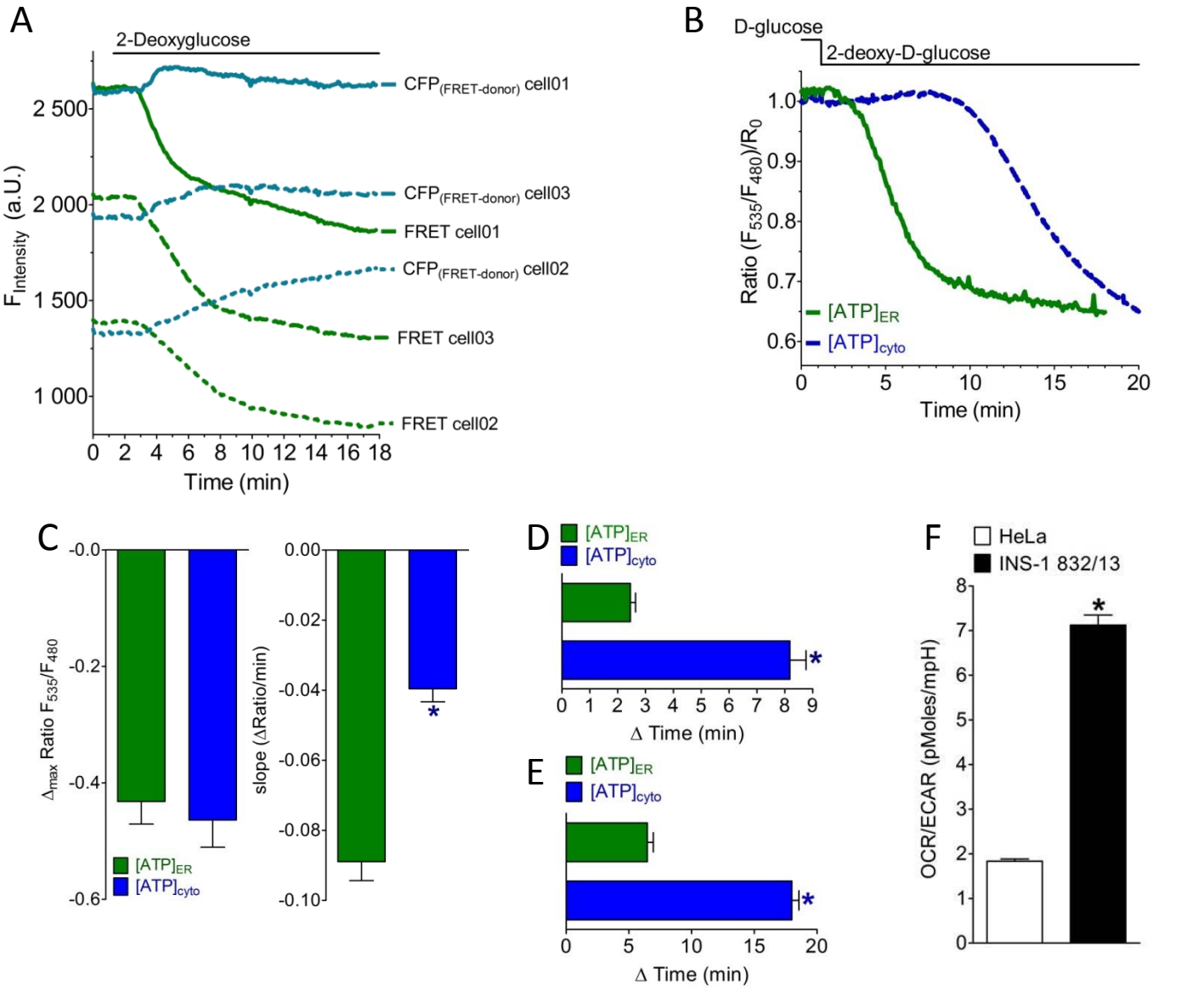

***ERAT4.01 Detects ER ATP Depletion in a Ratiometric Manner and Indicates Different Kinetics between ER and Cytosolic ATP Changes*.**

(A) Representative tracings of three different cells showing both, CFP (light blue curves) and FRET recordings (green curves) in HeLa cells upon treatment with 10 mM 2-deoxy-D-glucose (2-DG). **(B)** Normalized ratio signals of ERAT4.01 (green curve) are compared with that of the cytosolic ATP probe, AT1.03 (blue dotted line) to assess the relative kinetics of $[ATP]_{ER}$ and $[ATP]_{cyto}$ upon treatment with 10 mM 2-DG in HeLa cells. **(C)** Columns represent the maximal drop in normalized ratio signals in response to 10 mM 2-DG of the ER-targeted ATP probe ERAT4.01 (green column, n=10) and the cytosolic ATP probe AT1.03 (blue column, n=13) in the left panel. Columns in the right panel show the respective maximal slopes of 2-DG-induced reduction in normalized ratios of ERAT4.01 and AT1.03 signals in HeLa cells. *P < 0.05 vs. respective data from ERAT4.01 signals. **(D)** Columns represent the onset time of the drop in ERAT4.01 (green column, n=10) and AT1.03 (blue column, n=13) signals upon treatment with 10 mM 2-DG. *P < 0.05 vs. respective data from ERAT4.01 signals. **(E)** Columns show the time to reach a steady state minimum upon treatment with 2-DG by both, ERAT4.01 (green column, n=10) and AT1.03 (blue column, n=13). *P < 0.05 vs. respective data from ERAT4.01 signals. **(F)** Comparison of the metabolic activities of HeLa and INS-1 832/13 cells. Columns represent the ratio between the oxygen consumption rate (OCR), a measure of the mitochondrial OXPHOS, and the extra cellular acidification rate (ECAR), a measure of anaerobic glycolysis, in HeLa (with column, n=46) and INS-1 832/13 (black column, n=46) cells using the Seahorse technology. *P < 0.05 vs. HeLa cells.

Figure S3

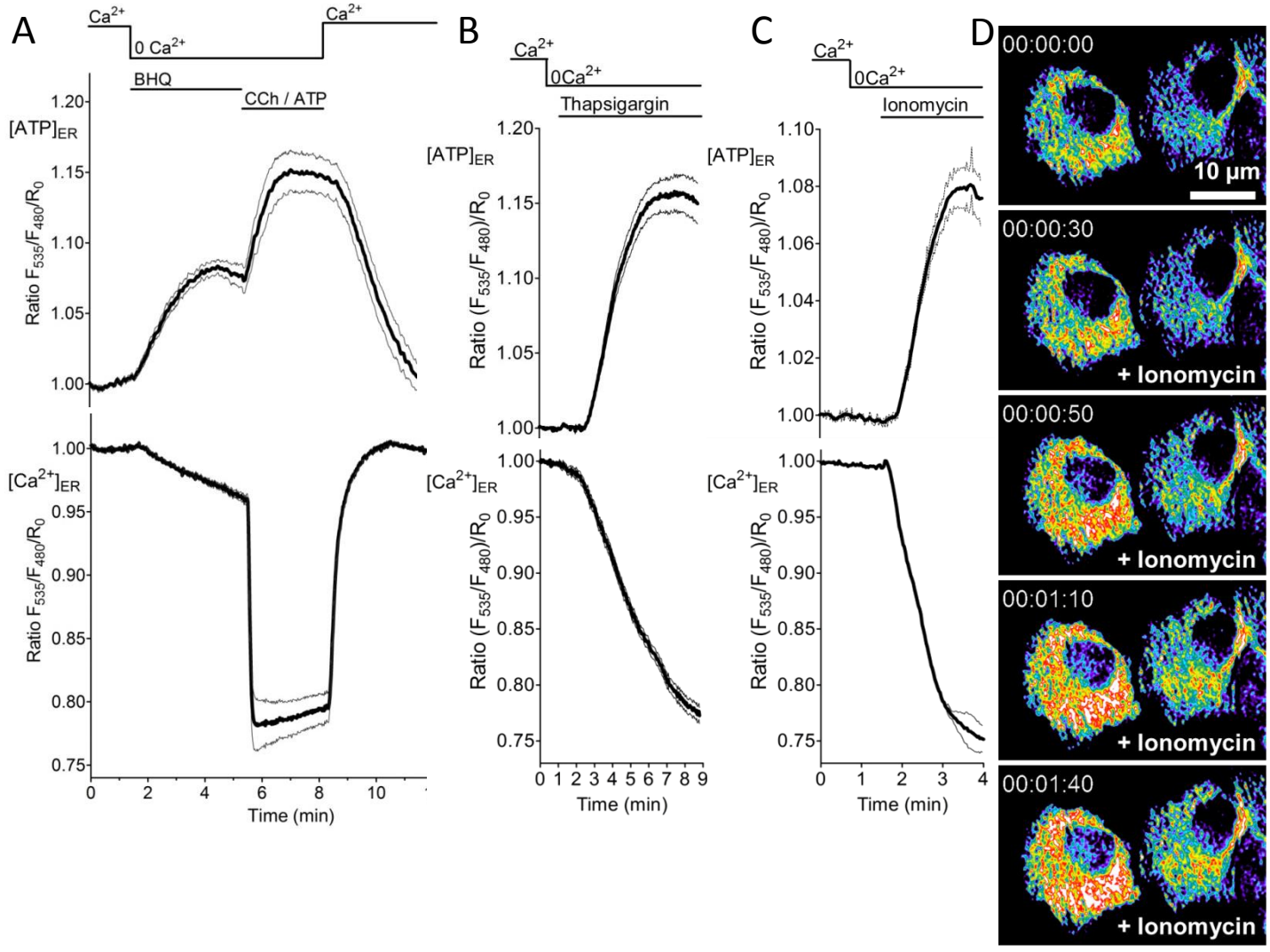

Independently of the Mode ER Ca^{2+} Mobilization Leads to an Increase of ATP Within the Lumen of the ER

(A) INS-1 832/13 cells expressing either ERAT4.01 (upper panel, n=7) or D1ER (lower panel, n=6) were treated with 15 µM BHQ and subsequently with mixture of 100 µM ATP and 100 µM carbachol (CCh). Curves represent normalized mean ratios ± SEM over time. **(B)** INS-1 832/13 cells expressing ERAT4.01 (upper panel, n=33) or D1ER (lower panel, n=34) were treated with 1 µM thapsigargin in the absence of Ca^{2+}. Curves represent normalized mean signal ratios ± SEM over time. **(C)** HeLa cells expressing ERAT4.01 (upper panel, n=41) or D1ER (lower panel, n=33) were treated with 2 µM ionomycin in the absence of Ca^{2+}. Curves represent normalized mean ratios ± SEM over time. **(D)** Representative pseudo-colored ratio (F_{535}/F_{480}) images over time of two HeLa cells expressing ERAT4.01 in which $[Ca^{2+}]_{ER}$ was mobilized with 2 µM ionomycin. Red colored pixels indicate high ratio values (>2), while blue pixels indicate low ratio values (<2).

Figure S4_I

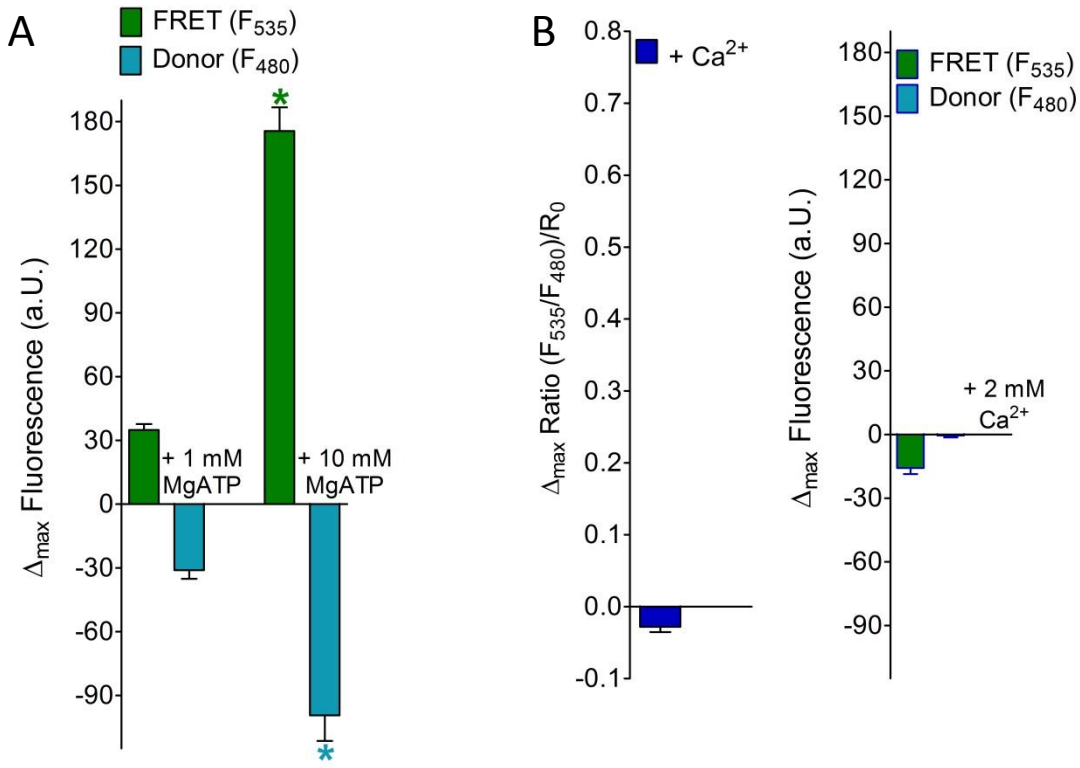

Characterization of genetically encoded ER targeted ATP probes (I)

(A) Columns represent changes of the fluorescence intensity of the FRET channel (green columns) and the donor channel (cyan columns) upon the addition of 1 mM MgATP (left column pairs, n=7) and 10 mM MgATP (right column pairs, n=17) to digitonin (10 µM) permeabilized HeLa cells INS-1 832/13 cells expressing ERAT4.01. **(B)** Effect of 2 mM Ca^{2+} on normalized ratio values (blue column, left panel, n=10) and the FRET and donor channel (right panel, n=10) of ERAT4.01 in permeabilized HeLa cells in the presence of 10 mM MgATP.

Figure S4_II

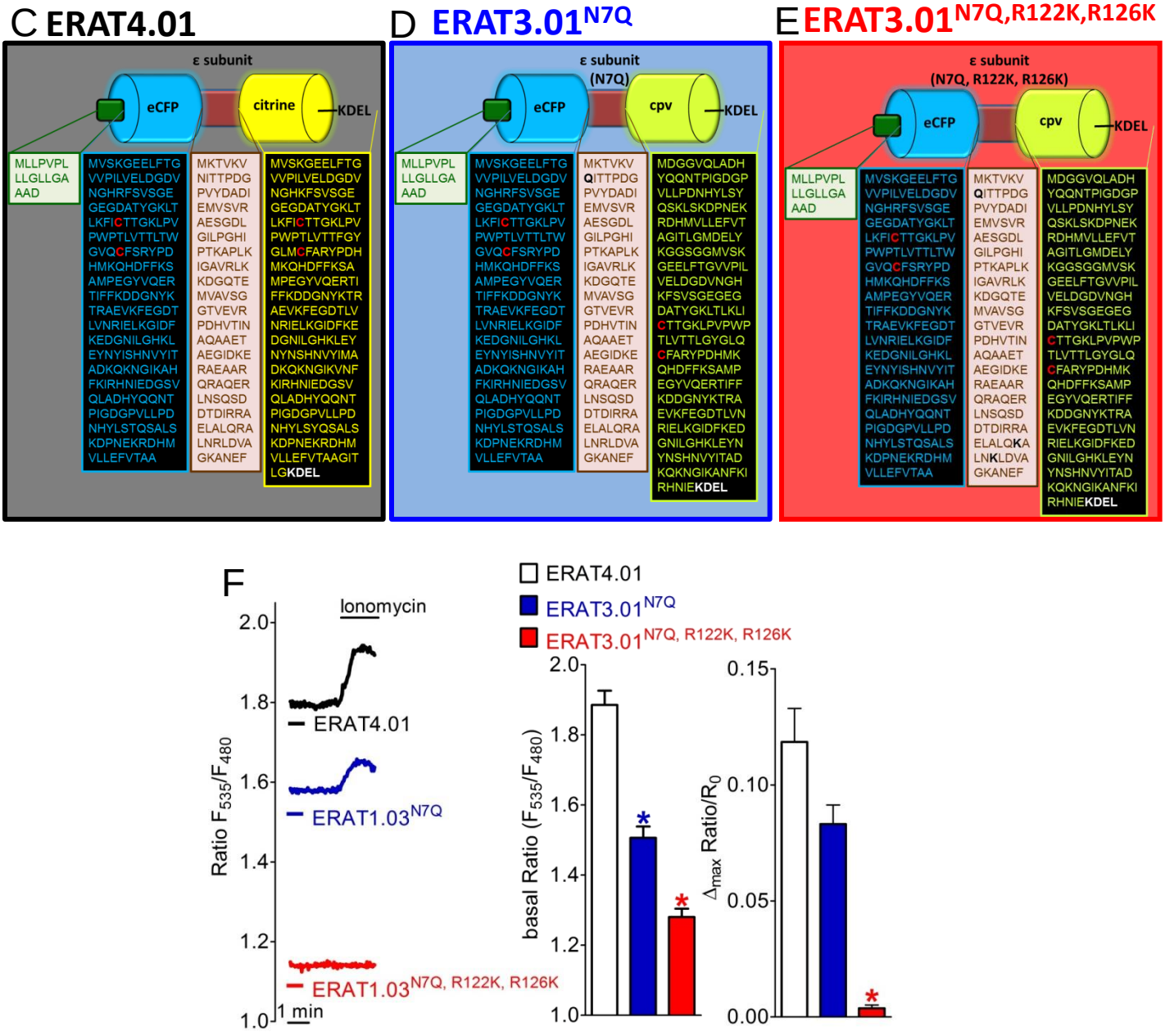

Characterization of genetically encoded ER targeted ATP probes (II)

(C) Schematic illustration of ERAT4.01 indicating the amino acid (AS) sequence and the positions of cysteins (C, red letters). **(D)** Schematic illustration and the AS sequence of the ERAT3.01^{N7Q} mutant, in which the putative glycosylation side within the ATP binding ε-subunit was mutated. **(E)** Schematic illustration of the ATP insensitive mutant ERAT3.01$^{N7Q,\ R122K,\ R126K}$ **. (F)** Representative responses (left panel) and statistics (middle and right panels) of FRET ratio signals of ERAT4.01 (black curve and white bars, n=18), ERAT3.01^{N7Q} (blue curve and columns, n=9), and the ERAT3.01$^{N7Q,\ R122K,\ R126K}$ mutant (red curve and columns, n=12). The genetically encoded probes were expressed in Hela cells that were treated with 2 µM ionomycin in the absence of extracellular Ca^{2+}.

Figure S4_III

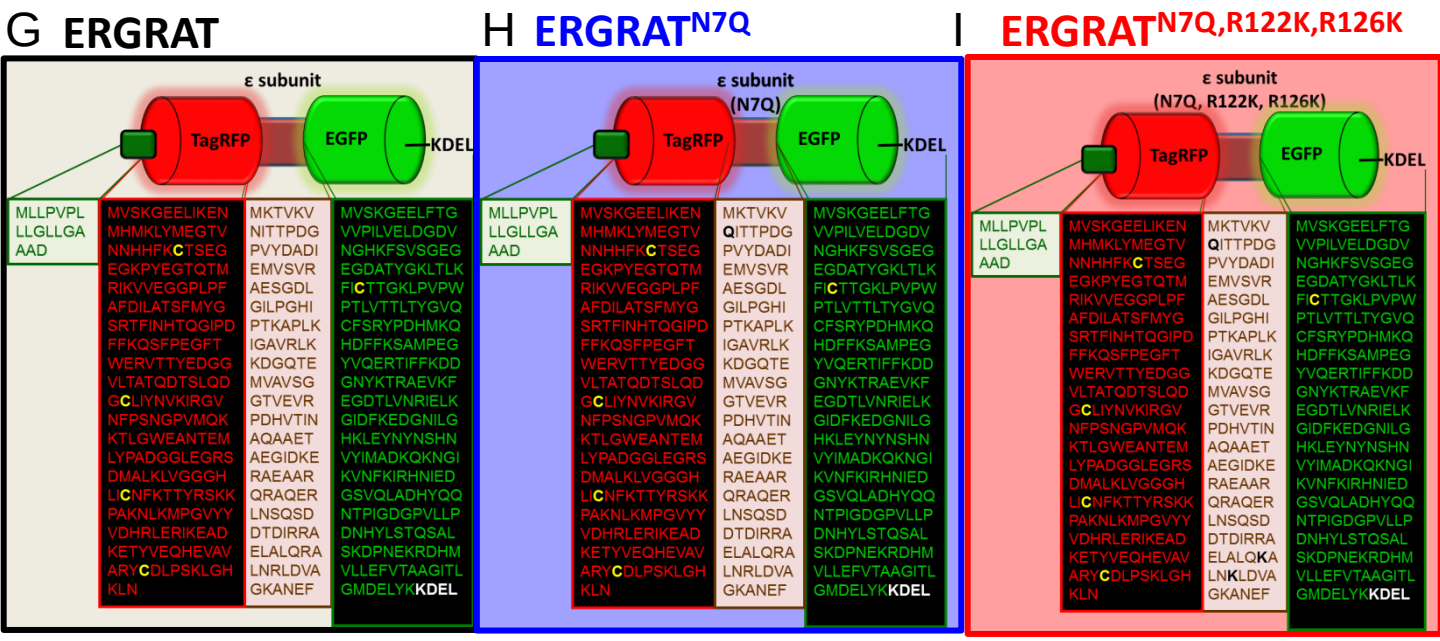

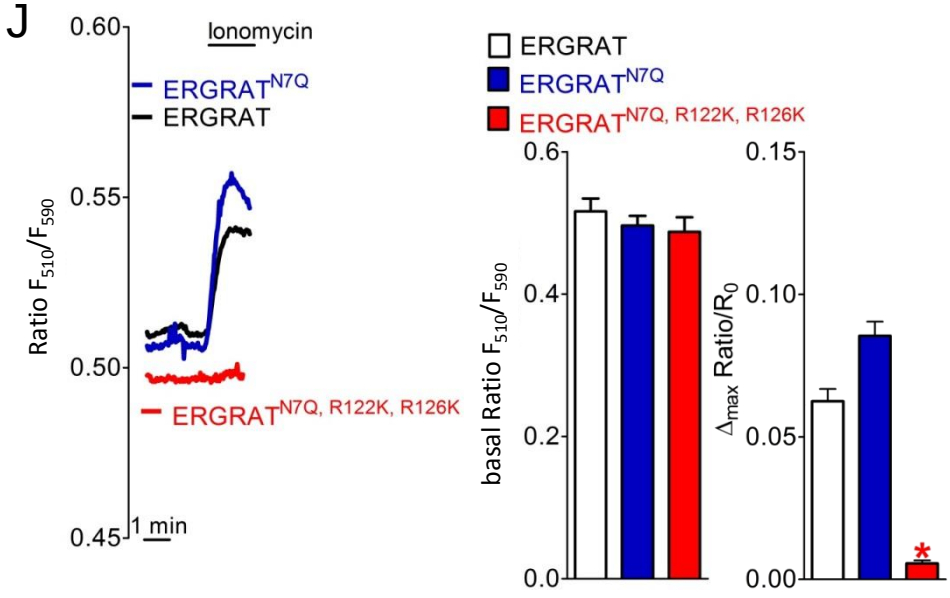

Characterization of genetically encoded ER targeted ATP probes (III)

(G) Schematic illustration of the red-shifted ER ATP sensor ERGRAT indicating the amino acid (AS) sequence and the positions of cysteins (C, yellow letters) within the FPs. **(H)** Schematic illustration and the AS sequence of the ERGRAT^{N7Q} mutant, in which the putative glycosylation side within the ATP binding ε-subunit was mutated. **(I)** Schematic illustration of the ATP insensitive red-shifted mutant ERGRAT$^{N7Q,\ R122K,\ R126K}$ **. (J)** Representative responses (left panel) and statistics (middle and right panels) of FRET ratio signals of the red-shifted ER ATP probes ERGRAT (black curve and white bars, n=12), ERGRAT^{N7Q} (blue curve and columns, n=14), and the ERGRAT$^{N7Q,\ R122K,\ R126K}$ mutant (red curve and columns, n=15). The genetically encoded probes were expressed in Hela cells that were treated with 2 µM ionomycin in Ca^{2+}-free medium on the microscope.

Figure S4_IV

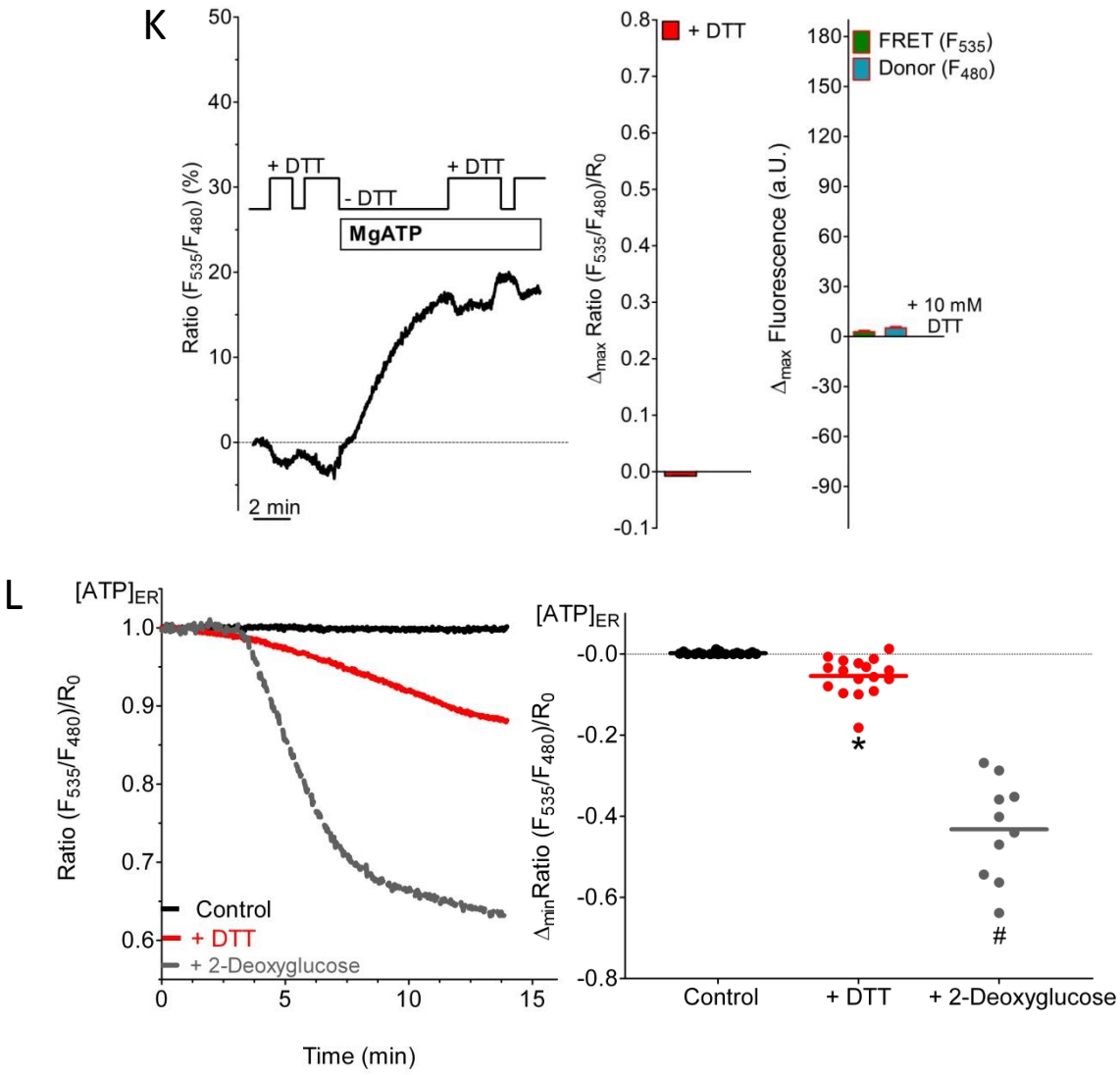

Characterization of genetically encoded ER targeted ATP probes (IV)

(K) Effect of 5 mM DTT on normalized FRET ratio signals (left and middle panel, n=8) and respective change of the fluorescence of the donor and FRET channel of ERAT4.01 in permeabilized HeLa cells in the absence and presence of 1 mM MgATP. The reducing effect of DTT on the ratio signals was independent of the presence of MgATP **(L)** Comparison between the reducing effect of 5 mM DTT and 10 mM 2-DG on the ERAT4.01 FRET signal in intact HeLa cells (control, n= 19; plus DTT, n=17 and plus 2DG, n=10).

Figure S5

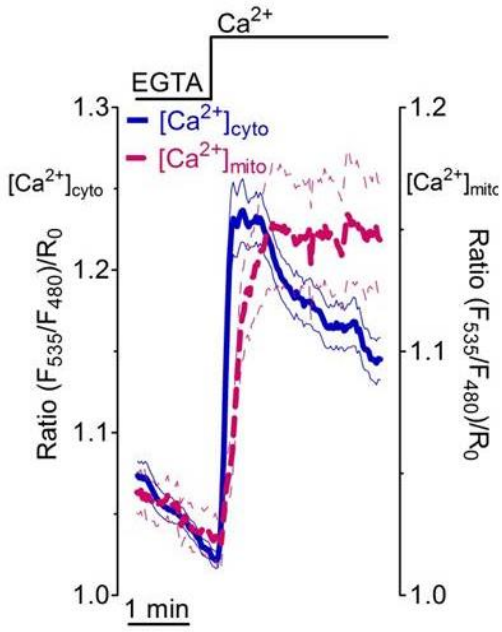

$[Ca^{2+}]_{cyto}$ is transferred to mitochondria upon SOCE in INS-1 cells

Average signals of $[Ca^{2+}]_{cyto}$ (blue curve, n=30) and $[Ca^{2+}]_{mito}$ (magenta dotted curve, n=20) in INS-1 832/13 cells upon SOCE. Cells expressed either the cytosolic cameleon D3cpv or the mitochondria-targeted Ca^{2+} probe 4mtD3cpv, respectively. SOCE was induced by ER Ca^{2+} depletion with 100 µM ATP and 15 µM BHQ in the presence of EGTA prior to Ca^{2+} addition.

Figure S6

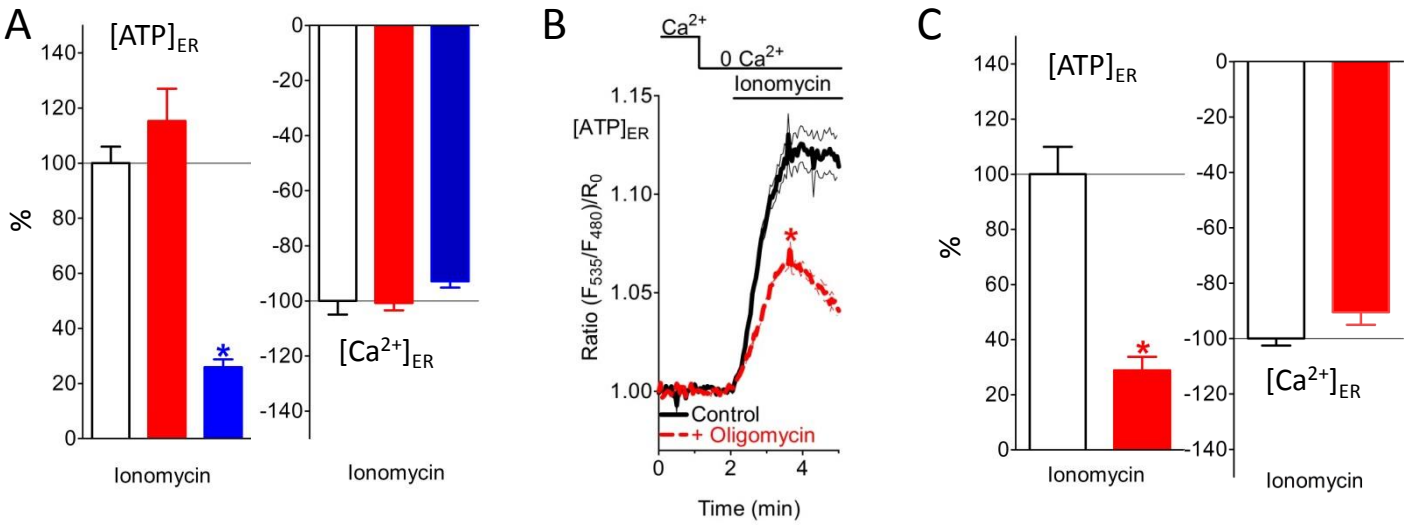

The Ca^{2+}-coupled ATP rise within the lumen of the ER requires ATP synthesis

(A) Columns represent the normalized changes in $[ATP]_{ER}$ (left columns) and $[Ca^{2+}]_{ER}$ (right columns) in control HeLa cells (white columns) and HeLa cells that were either treated with 2 µM oligomycin A (red column) or 2-DG (blue columns) prior to Ca^{2+} mobilization by 2 µM ionomycin (left panel, Control n=21; plus oligomycin A n=23; plus 2-DG n=8 for $[ATP]_{ER}$; and Control n=11; plus oligomycin A, n=15; plus 2-DG, n=12 for $[Ca^{2+}]_{ER}$ shown in the right panel). *P < 0.05 vs. controls. **(B)** Long Term Inhibition of the mitochondrial ATP synthase partially reduced the Ca^{2+}-coupled ER ATP Signal in HeLa cells. Cells were incubated with 2 µM oligomycin A (red dotted curve) for 30 minutes before recording. ERAT4.01 signals upon ER Ca^{2+} release induced by 2µM ionomycin are presented for cells treated with DMSO as control (black curve, n= 17) or treated with oligomycin A (red dotted curve, n=17). Curves represent normalized mean ratios ± SEM over time. *P < 0.05 vs. control. **(C)** Columns representing the changes in $[ATP]_{ER}$ (left columns) and $[Ca^{2+}]_{ER}$ (right columns) in INS-1 cells treated with 2 µM oligomycine A (red column) as compared to untreated controls (white columns). Ca^{2+} was mobilized by 2µM ionomycin in Ca^{2+}-free medium (left panel, Control n=10; plus oligomycin A, n=10 for $[ATP]_{ER}$; and Control, n=52; plus oligomycin A, n=13 for $[Ca^{2+}]_{ER}$). *P < 0.05 vs. respective controls.

Figure S7_I

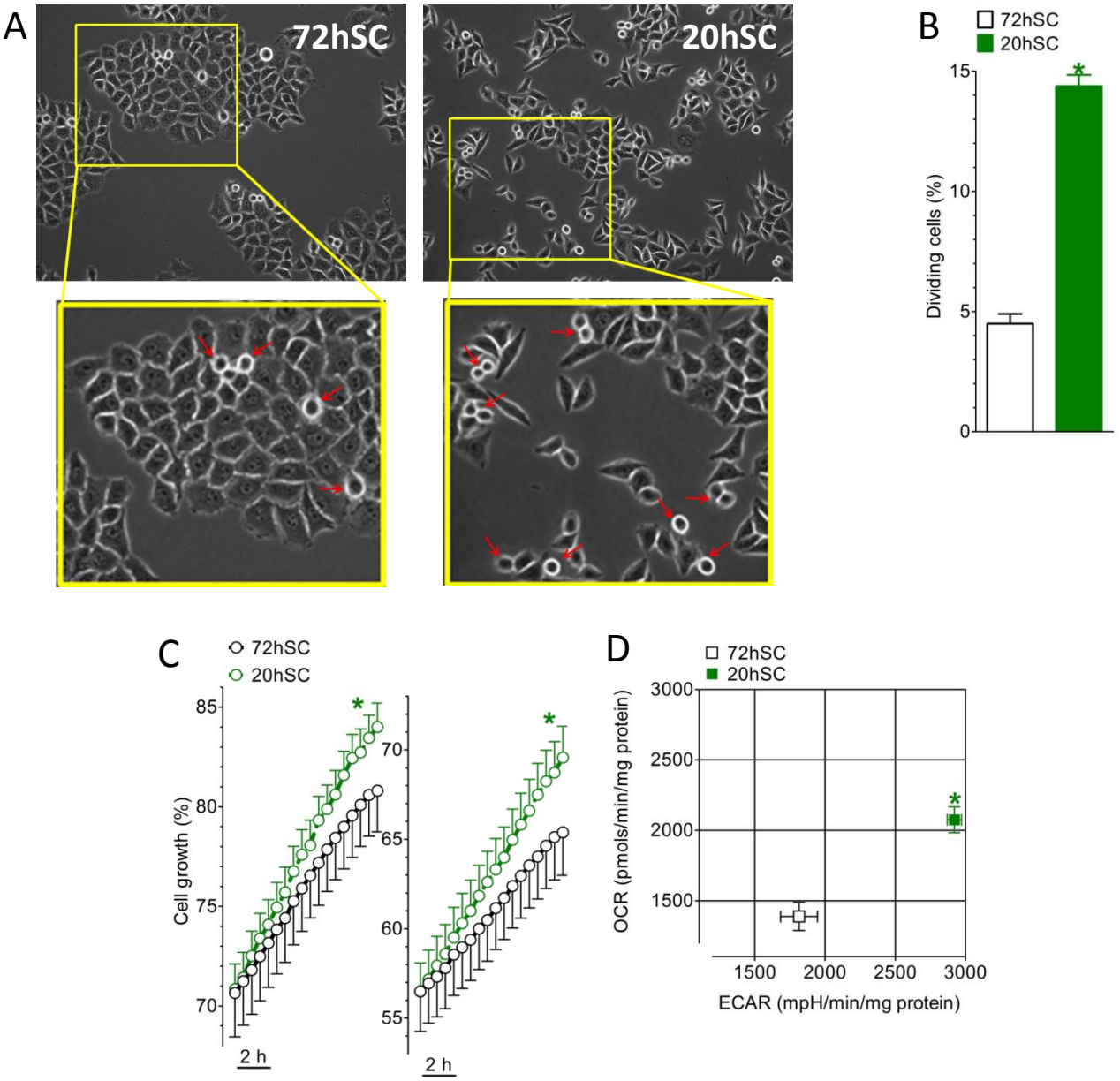

The Metabolic Status of HeLa Cells Depends on the Growth Rate, Glucose Availability and is Regulated by AMPK (I)

(A) Representative phase contrast images of HeLa cells taken by Cell-IQ© device (ChipmanTechnology, Tampere, Finland). Cells were either split 72 h (72hSC) or 20 h (20hSC) before monitoring. In the images with lower magnification the dividing cells are indicated by red arrows. **(B)** The image series over time from panel A was analyzed with Cell-IQ© Analyser software to differentiate dividing and non-dividing cells. The percentage of dividing cells in the two groups (72hSC, white column, n=6 and 20hSC, green column n=6) were compared for 8.5 h. *P < 0.05 vs. 72hSC. **(C)** Cell growth was estimated from the image series at randomly chosen areas by calculating the confluence using Cell-IQ© Analyzer software. Cells were monitored for 20 hours at two different initial confluences, i.e. ~70% (left panel) and ~55% (right panel) (n=6 for both conditions). *P < 0.05 vs. 72hSC. **(D)** Basal cellular metabolic profiles of 72hSC and 20hSC were analyzed on a Seahorse XF96 extracellular flux analyzer. Absolute oxygen consumption rate (OCR) and extracellular acidification rate (ECAR) were normalized to total cellular protein. As indicated the 20hSC (green square, n=24) had a higher overall metabolic rate as compared to 72hSC (white square, n=24).*P < 0.05 vs. 72hSC.

Figure S7_II

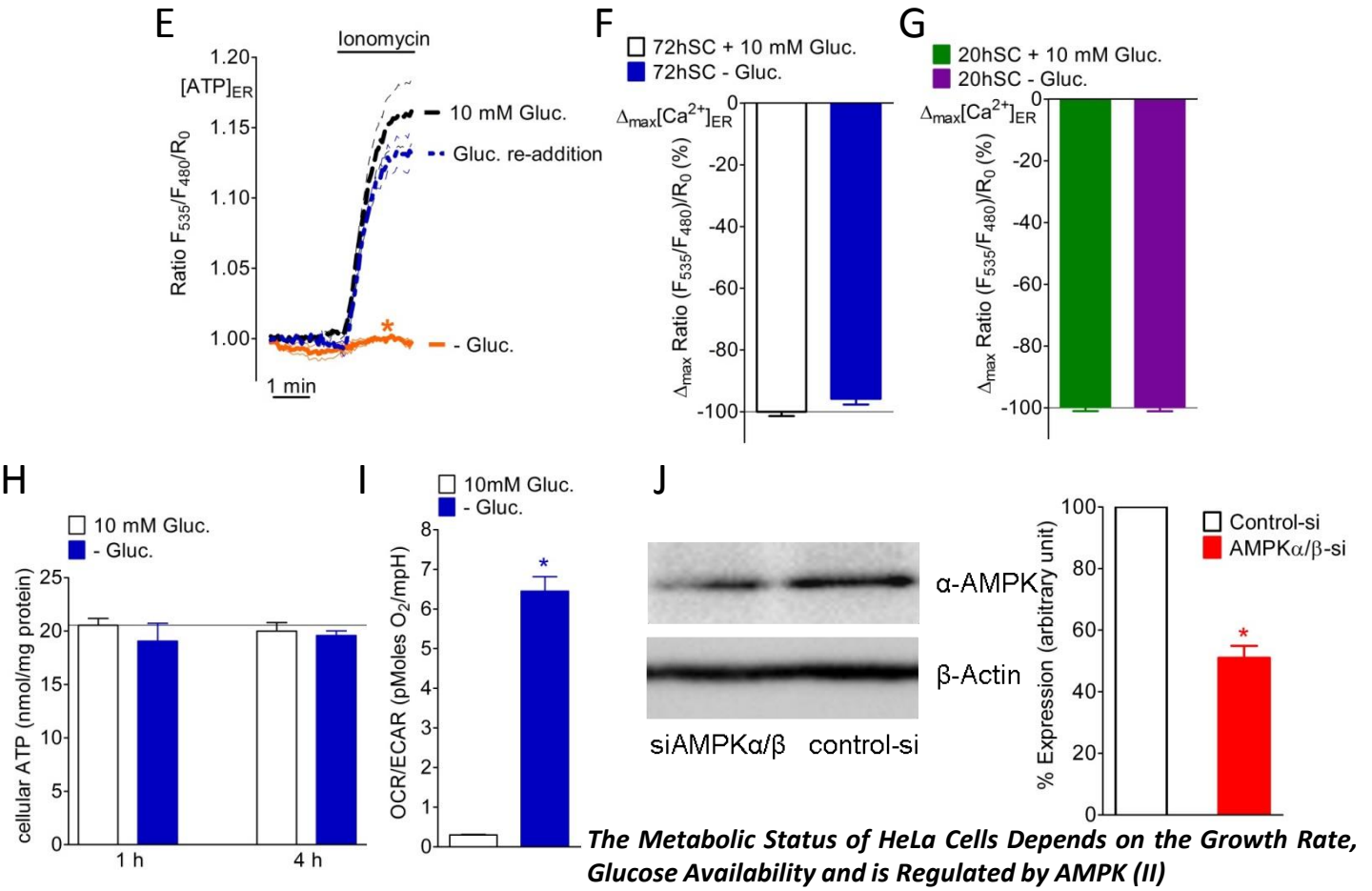

The Metabolic Status of HeLa Cells Depends on the Growth Rate, Glucose Availability and is Regulated by AMPK (II)

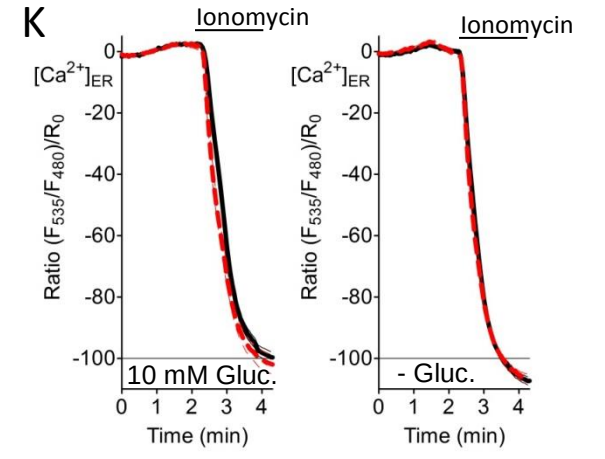

(E) The effect of glucose availability on the Ca^{2+}-coupled ER ATP transfer was analyzed by removing the glucose in the medium and measuring ERAT4.01 signals in response to 2 µM ionomycin in Ca^{2+} free medium. 10mM glucose (10 mM Gluc) was continuously present in the medium during ERAT4.01 signal recordings over time in controls (black dotted curve, n=13), while it was removed for 4 minutes (-Gluc) prior to stimulation with ionomycin (orange curve, n=9). In a glucose re-addition experiment (Gluc re-addition, n=11) cells were deprived of glucose for 4 minutes followed by re-addition for another 4 minutes before stimulation with ionomycin (blue dotted curve).*P < 0.05 vs. 10mM Gluc containing cells. **(F)** Columns represent relative change of $[Ca^{2+}]_{ER}$ in 72hSC in response to 2 µM ionomycin with 10 mM (n=21) or without glucose (n=17), as indicated in Figure 7C.

(G) Columns represent relative change of $[Ca^{2+}]_{ER}$ in 20hSC in response to 2 µM ionomycin with 10 mM (n=18) or without glucose (n=18), as indicated in Figure 7D. **(H)** Columns represent the average total cellular ATP amount normalized to the individual protein content in control HeLa cells (cells cultured in 10 mM glucose, white columns, n=4) and HeLa cells that were kept in glucose-free medium for 1h and 4h, respectively (blue columns, n=4). **(I)** The effect of glucose starvation on the rate of OXPHOS was assessed by calculating the ratio between OCR and ECAR (plus glucose, white column, n= 15; without glucose, blue column, n=15). *P < 0.05 vs. 10 mM Gluc. **(J)** Representative blot showing the knock-down efficiency of AMPKα/β and statistics (siControl, white column, n=3; siAMPKα/β, red column, n=3).*P < 0.05 vs. siControl. **(K)** D1ER signals in the presence of 10 mM glucose (left panel) in control (black curves, n=23) and AMPKα/β-siRNA (red curves, n=20) treated HeLa cells in response to 2 µM ionomycin in Ca^{2+}-free medium. Respective D1ER signals of glucose starved cells are shown in the right panel (Control, n=32; siAMPKα/β, n=25).